2003 REU in Green Bank, West Virginia

Radio Point Source Contamination in Galaxy Clusters

Regina M. Flores

Columbia University,Barnard College,3001 Broadway#4076,NY,NY,10027

Advisor: Brian S. Mason

National Radio Astronomy Observatory,P.O. Box 2,Green Bank,WV,24944

ABSTRACT

Observations of the Cosmic Microwave Background (CMB) with the Cosmic Background Imager (CBI) have revealed radio foreground signals that limit the accuracy of measurements of the anisotropic properties of the CMB such as the Sunyaev-Zeldovich Effect. By comparing CBI data to NVSS (and PMN) data, accurate counts of the number of radio sources in low redshift galaxy clusters were made. It was determined that at 30 GHz there are 1.4 ± 0.3 sources brighter than 30mJy in the sky per deg^2 in fields containing galaxy clusters. Comparing these results to the number of radio sources at random in the sky at 30 GHz (Mason et al.) a 1.38σ difference was found. We therefore do not detect a strong difference in the number of radio sources at 30 GHz in galaxy cluster fields.

1. INTRODUCTION

The Cosmic Microwave Background (CMB), found in all directions in the sky, is the primordial radiation from the Big Bang and radiates at about 3K. Although it was once thought to be isotropic, it is known today that the CMB actually has anisotropic properties. An example of such anisotropies is the Sunyaev-Zeldovich Effect (SZE). When a photon attempts to pass through the hot gas in between clusters of galaxies, whose total masses are about 100 trillion solar masses, it is scattered by reverse Compton scattering thus boosting its energy and distorting its spectrum. In 1970 two scientists, Sunyaev and Zeldovich, first predicted this phenomenon and, in doing so, revolutionized the study of cosmology. Perhaps one of the most important results from the SZE is the possibility of a direct measurement of the Hubble Constant, H_0, and therefore the ability to determine with more accuracy the age and size of the universe.

2. THE COSMIC BACKGROUND IMAGER

Fig. 1.— Image of the CBI (http://www.astro.caltech.edu/~tjp/CBI/)

The Cosmic Background Imager (Figure 1) is located in the Chilean Andes Mountains at 16,700 feet. This CMB specific instrument, meaning that it functions solely for performing CMB experiments, is a 13 element interferometer operating from 26 to 36 GHz. At such high altitudes the dry climate reduces "atmospheric brightness fluctuation"(Mason et al.) thus allowing for a very high sensitivity. The CBI is especially useful for observing SZE because it allows for relatively short baselines (about 1-2 meters). However, measuring the SZE does present certain challenges due to the limitations in the instrument. Such challenges are a result of contaminates like signals from the ground, atmospheric emission, and radio sources in the foreground. To address the latter challenge, radio source contamination, data can be taken at longer baselines, of 5-6 meters, and subtracted from the short baseline data.

3. THE EXPERIMENT

In this paper we attempt to find the number of radio point sources in low red-shift galaxy cluster fields and then to compare this to the number of radio sources at random in the sky. The hope is that the results of this experiment will provide a statistical correction to the SZE CBI data taken at short baselines. The data was taken by the CBI collaboration over the period of December, 1999 to December, 2001.

4. DATA REDUCTION

4.1. *DIFMAP and the CLEAN Process*

The data reduction was performed in DIFMAP which is a program that specializes in "difference mapping". The CLEAN process, a function within DIFMAP, allows the user to subtract a model of a given source from a "dirty map" thus creating what is known as a "residual map". By iteratively subtracting model sources, a "clean map" is eventually created. In each iteration a delta function is added to the model. For data reduction purposes the following selections were made: left circular polarization was used, griding weights were scaled by errors raised to the power -2, and the UV range was 0.3 to 1 Kλ. For the CLEAN routine 100 iterations were made at a gain of 0.1, and the cutoff was set to 5 times the noise.

4.2. *Procedure: Locating Radio Point Sources*

There were a total of 19 fields of galaxy clusters used in this experiment. Each field was analyzed above a 5σ noise cut-off[1]. Table 1 shows the noise levels of each field. It is possible to locate the radio source contamination by analyzing the values of each pixel in the map, where pixel values represent flux density, and checking if the value is 5 times greater than or equal to the noise. Cross marks are placed on those pixels which are above or equal to 5σ. This was first done manually using a command line routine in the DIFMAP environment. Figure 2a shows a typical dirty map from the CBI, in this case galaxy cluster A401. The large, circular contaminants in the center of the dirty map are clues that those pixels are above 5σ. However, point sources are not always so easy to see with the naked eye. That is why it is imperative to cross check the manual method with the CLEAN method. Figure 2b

[1]A 4σ noise cut-off was eliminated after the comparison process with NVSS and PMN as there were too often sources in the maps that did not correlate with the "known" cataloged sources.

shows a CLEAN map of the same cluster. The cross marks indicate where CLEAN located the sources. Red and orange crosses represent negative flux densities, and green and yellow represent positive flux densities. The discoloration of the cross marks is due to the fact that for very bright sources, about ±30 mJy, DIFMAP places many, 2 or 3, cross marks. The user must go through by hand to verify that for one point source there is only one cross mark. In doing so, a yellow mark is placed for positive sources, and an orange mark is placed for negative sources. After this "massaging" of the maps, the manual method and the CLEAN method matched for all 19 galaxy clusters. Once this check had been finalized, another check was made to verify the validity of our 5σ noise threshold. A comparison of our radio point sources to cataloged radio point sources was made with NRAO/VLA Sky Survey (NVSS) for sources north of a declination of -40° and with Parkes-MIT-NRAO Survey (PMN) for all other sources. For a given field either the NVSS or PMN database was searched for all radio sources within 100 arc minutes of the field center. The sources were then uploaded in DIFMAP onto the field map in order to visually match the "cleaned" sources to the "known" sources. A numerical check was also made by comparing the model file of a given field, containing right ascension (R.A) and declination (DEC) of the field center, with the R.A and DEC from the NVSS or PMN database. Figure 3 shows the 100 arcmin region where radio sources were found. When comparing Figure 2b to Figure 3, it is clear that the "known" sources match the "clean" sources.

5. STATISTICAL ANALYSIS

Having verified that the radio sources found in the data were in fact real, "known" sources, they were then cataloged in a table, see Table 2, along with other information found in the DIFMAP model file such as flux density. A total of 38 sources were initially identified. However, since only positive sources are used in the NVSS and PMN databases, the negative sources in our data had to be eliminated. Therefore, the 27 sources counted in this analysis include only positive sources. To determine the true flux density, a correction for the CBI beam had to be made. Equation 1 shows the necessary correction where $\sigma^2 = \frac{45'}{\sqrt{8ln2}}$:

$$S_{obs} = S_{true} * P(r) = S_{true} * e^{\frac{-r^2}{2\sigma^2}} \tag{1}$$

To determine the number of sources greater than a given flux density in an area in the sky, the normalization, N_0, from Equation 2 must be found.

$$N(> S) = N_0(\frac{S}{S_0})^{\lambda} \tag{2}$$

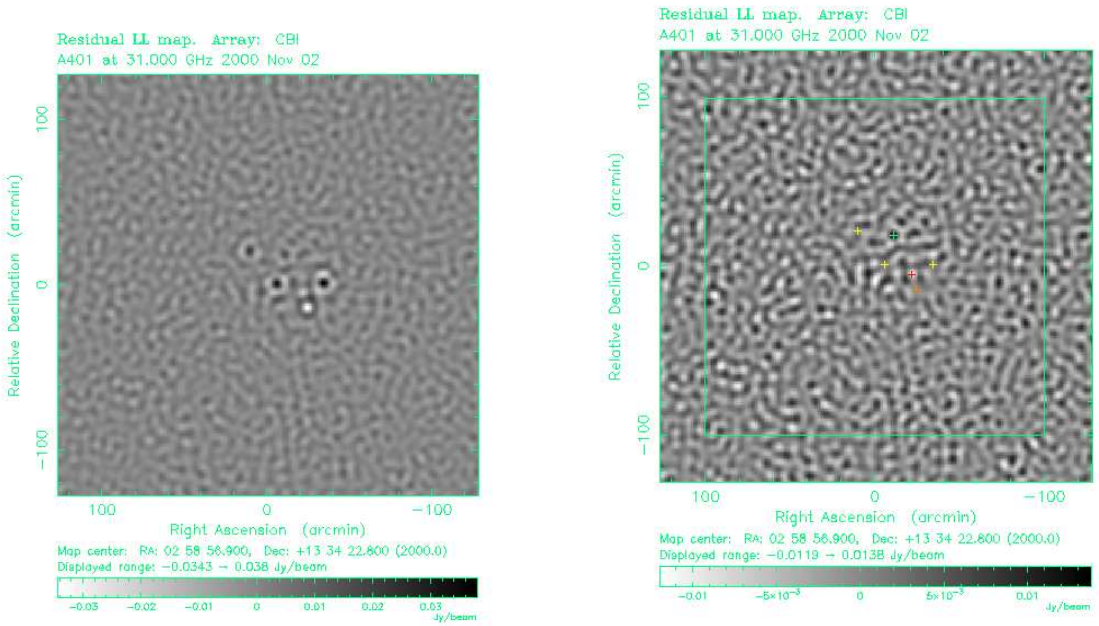

Fig. 2.— Figure 2a (left): Dirty map of A401. Large contaminants in the center of map show possible radio point sources. Figure 2b (right): CLEAN map of A401 identifying the radio point sources above 5σ.

Figure 4 shows the distribution of the area over which a source can be found in the sky. For this plot, the area was calculated using all 19 fields and all 27 sources. In the following equation, n denotes noise (subscript k), and S denotes flux density (subscript i):

$$A(S_i, n_k) = \pi * (-730.36) \ln \frac{5n_k}{S_i} \tag{3}$$

A program was written in the IDL programming language to find the normalization of Equation 2. The first task was to generate a routine to satisfy the equation and calculate the normalization. The following equation is an alternative way to write Equation 2:

$$N(> S_j) = \sum_{S_i > S_j} \frac{1}{A(S_i)} = \sum_{S_i > S_j} \frac{1}{\sum_k (-730.36)\pi \ln \frac{5n_k}{S_i}} \tag{4}$$

Flux density S_j was randomly chosen to be between 15 and 300mJy. Note that i is for all the flux densities associated with each source, j is for all the randomly chosen flux densities,

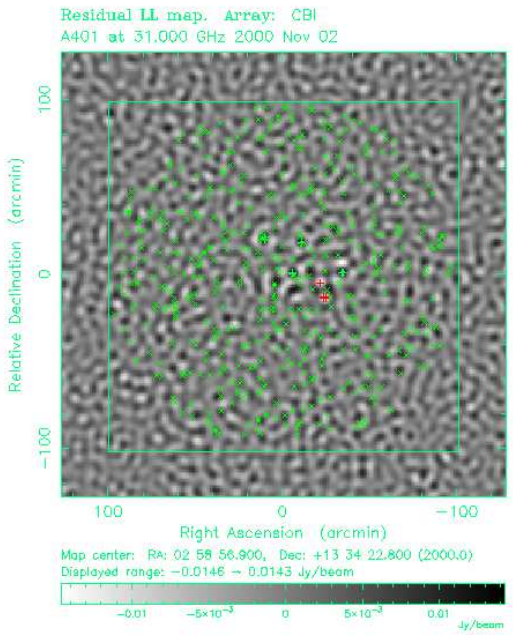

Fig. 3.— Shows the sources found in NVSS within 100 arcmin of R.A 02:58:56.90 and DEC +13:34:22.80.

and k is for each field. From Equation 2, we see that taking the log of both sides gives

$$log(N(>S)) = \lambda log(S) + log(\frac{N_0}{S_0^\lambda}) \tag{5}$$

Figure 5 shows a log/log plot of the number of sources greater than S_j per arcmin^2 as a function of S_j where the slope of the line is given as λ. The value for λ, found by a linear fit, was calculated as -1.4. From Equation 2, setting both S and S_0 to 30mJy and converting N(>30mJy) to deg^{-2}, we get a value of N_0 of 1.4 deg^{-2}.

6. RESULTS

From the statistical analysis it was determined that there are 1.4 $\pm$0.3 radio sources brighter than 30mJy in the sky per deg^2 as shown in Equation 6.

$$N(>S) = 1.4 \pm 0.3 deg^{-2}(\frac{S}{30mJy})^{-1.4} \tag{6}$$

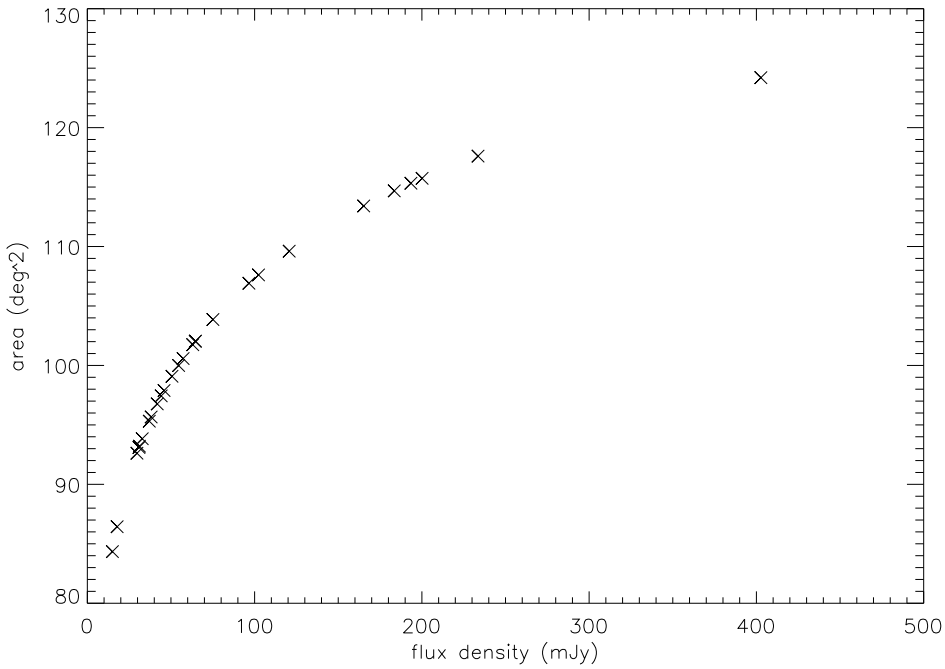

Fig. 4.— Area as a function of flux density.

This number includes the contribution both from the sources associated with the galaxy cluster as well as the sources that would be there if there were no cluster. Correcting the Mason et al. number for a 30mJy threshold flux density yields Equation 7.

$$N(>S) = 0.9 \pm 0.2 deg^{-2} (\frac{S}{30mJy})^{-1.0} \tag{7}$$

Comparing Equation 6 to Equation 7, a 1.38σ difference was found. Since this value is below 2σ, we can see that this value is not highly significant, and, therefore, there is inconclusive evidence as to whether or not this value is due to noise. Therefore we see that, in terms of this result, the number of radio sources in clusters per deg^2 is roughly the same as the number of radio sources per deg^2 at random in the sky. Correcting the Cooray et al. value for a 30mJy threshold flux density yields Equation 8.

$$N(>S) = 2.25 \pm 0.7 deg^{-2} (\frac{S}{30mJy})^{-0.96 \pm 0.14} \tag{8}$$

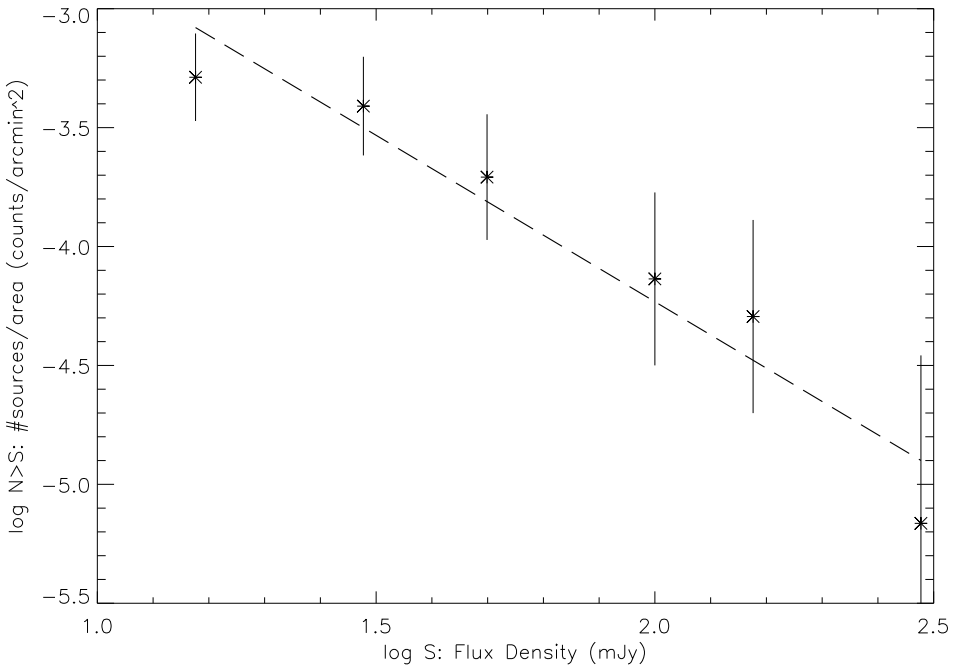

Fig. 5.— Plotting the log of Equation 2 where the slop of the line is λ.

Comparing this to Equation 6, a 1.11σ difference was found. Again, we see that this falls well below 2σ, and we can conclude that this value is not highly significant. Recomputing Equation 8 to account for the λ error bar, the following was found:
For the (+) error:

$$N(>S) = 1.39 \pm 0.4 deg^{-2} (\frac{S}{30mJy})^{-0.82} \tag{9}$$

For the (-) error bar:

$$N(>S) = 3.62 \pm 1.07 deg^{-2} (\frac{S}{30mJy})^{-1.1} \tag{10}$$

Therefore, in the comparison of the result found in this paper to the Cooray result, the uncertainty in the power law dominates.

7. CONCLUSION

Identifying radio source contamination in the CBI SZE data not only provides a statistical correction to the data but, perhaps more importantly, helps in understanding the measurements of the Hubble constant, H_0, from the SZE data. Although it is possible to directly subtract those sources that are bright enough to be detected, such as the ones found in this paper, there are many sources that are found below the noise cut-off point and therefore bias a measurement of H_0. However, we can extrapolate just below our detection threshold and correct for those sources as well.

We also wish to address the Cooray et al. claim that there are 4-7 times as many sources in galaxy clusters as in random fields in the sky. In other words, we wish to address the question as to whether or not radio point source "clusters" are intrinsic to radio galaxy clusters. Comparing our sample of radio sources in clusters to four times the Mason et al. sample of random sources, it was determined that there is a 2.6σ difference. Since this difference is above the 2σ confidence threshold, we can conclude that this result is significant and therefore contrary to the prediction that there are more sources at random in the sky than in galaxy clusters. However, when comparing the Cooray sample of radio sources in clusters to four times the random Mason et al. sample, a 1.27σ difference was found. This result is not highly significant and therefore does agree with the Corray et al. findings. We conclude, therefore, that there is indecisive evidence as to whether there are more radio sources in galaxy clusters or at random in the sky. Further investigation of this problem is not possible in the scope of a summer research project but would be the next step in fully examining a correction to the CBI SZE data.

I wish to thank the staff at NRAO, Green Bank, in particular R.J. Maddalena, for their support of my REU position. I would also like to thank NRAO, Charlottesville, in particular J.E. Hibbard, for making this experience possible. I would also like to acknowledge the National Science Foundation and thank all those who make the REU Program possible. A very special thank you is awarded to B.S. Mason for his continued enthusiasm and willingness to assist me in pursuing my scientific goals.

REFERENCES

Birkinshaw, M. 1998, Phy. Rep., submitted

Cooray, A. R., Grego, L., Holzapfel, W. L., & Joy, M.,Carlstrom, J. E 1997, ApJ, 115, 1399

Mason, B. S. 1999, Ph.D. thesis, University of Pennsylvania

Mason, B. S. et al. 2003, ApJ, 591, 540

Shepherd, M. C, 1997, ASP Conference Series, Vol.125,
http://www.cv.nrao.edu/adass/adassVI/shepherdm.html

Udomprasert, P. S., Mason, B. S, Readhead, A. C. S 2000, Astro. Ph., 0012248, 1

Udomprasert, P. S., Mason, B. S, Readhead, A. C. S 2000, Conference Proceedings

Table 1. Noise Values

Field/Name	Noise (Jy)
Abell 1651	0.00266
Abell 2029	0.00319
Abell 2597	0.00340
Abell 3558	0.00260
Abell 3571	0.00225
Abell 399	0.00295
Abell 401	0.00294
Abell 478	0.00336
Abell 754	0.00284
Abell 85	0.00261
Abell 1650	0.00304
Abell 2384	0.00234
Abell 3112	0.00268
Abell 3158	0.00244
Abell 3266	0.00242
Abell 3667	0.00248
Abell 3827	0.00228
Abell 3921	0.00436
Abell 4010	0.00371

Table 2. Subtracted Sources

Field/Name	Beam Size (arcmin)	$S_{observed}$ (Jy)	r (arcmin)	R.A	Decl.	Redshift	S_{true} (Jy)
A1651.1	4.49	0.0418	17.82	12:59:48.54	-03:54:34.8	—	0.0646
A2029.1	3.95	0.1425	27.54	15:11:41.19	+05:18:09.4	0.084	0.4026
A2029.2	3.95	0.0654	16.86	15:09:47.46	+05:45:31.8	0.098	0.0966
A2597.1	4.26	0.0417	1.00	23:25:19.82	-12:07:28.6	0.082	0.0417
A3558.1	3.98	0.0627	30.97	13:30:19.07	-31:22:58.8	1.326	0.2335
A3558.2	3.98	0.0134	8.84	13:28:31.49	-31:35:03.8	—	0.0149
A3571.2	3.95	0.0136	33.70	13:46:28.76	-32:20:51.8	—	0.0645
A3571.3	3.95	0.0154	21.88	02:58:10.39	+13:51:50.4	—	0.1934
A401.4	4.20	0.0362	6.059	02:58:31.89	+13:34:17.4	0.064	0.0381
A401.5	4.20	0.0219	23.21	02:59:37.57	+13:54:36.6	0.074	0.0458
A401.6	4.20	0.0169	21.11	02:59:39.33	+13:55:24.3	0.074	0.0311
A754.1	4.19	0.0440	10.10	09:08:27.44	-09:32:35.9	—	0.0506
A754.2	4.19	0.0230	25.05	09:09:26.99	-09:22:49.4	0.059	0.0545
A754.3	4.19	0.0284	17.93	09:09:30.98	-09:23:10.5	—	0.0441
A754.4	4.19	0.0176	20.26	09:09:32.16	-09:22:18.7	—	0.0308
A85.1	4.16	0.0154	10.25	00:42:30.38	-09:22:04.0	0.056	0.0178
A1650.1	4.10	0.0573	8.32	12:59:06.60	-01:50:58.1	—	0.0630
A1650.2	4.10	0.0173	21.61	12:57:14.68	-01:50:53.1	—	0.0328
A2384.1	3.95	0.0997	11.80	21:51:51.00	-19:46:06.0	0.424	0.1206
A3112.1	4.23	0.1834	0.52	03:17:58.60	-44:14:16.0	—	0.1835
A3112.2	4.23	0.0387	26.62	03:16:38.30	-43:51:23.0	0.062	0.1023
A3112.3	4.23	0.0167	29.97	03:20:24.50	-44:00:33.0	—	0.0572
A3266.1	4.20	0.1702	10.86	—	—	—	0.2001
A3667.1	3.96	0.0333	8.71	20:11:27.90	-56:44:01.0	0.053	0.0370
A3667.2	3.96	0.0473	18.35	20:14:01.60	-57:01:10.0	0.057	0.0751